miR-17-92 functions as an oncogene and modulates NF-κB signaling by targeting *TRAF3* in MGC-803 human gastric cancer cells

FEI LIU[1], LI CHENG[2], JINGJING XU[3], FENG GUO[4] and WEICHANG CHEN[1]

Departments of [1]Gastroenterology and [2]Oncology, and [3]Center for Clinical Laboratory,
The First Affiliated Hospital of Soochow University, Suzhou, Jiangsu 215006; [4]Department of Oncology,
The Affiliated Suzhou Hospital of Nanjing Medical University, Suzhou, Jiangsu 215001, P.R. China

Abstract. The *miR-17-92* cluster plays either an oncogenic or anti-oncogenic role in cancer progression in diverse human cancers. However, the underlying mechanisms of the *miR-17-92* cluster in gastric cancer have not yet been fully elucidated. In this study, the function of the *miR-17-92* cluster in diverse aspects of MGC-803 gastric cancer cells was systematically elucidated. The enforced introduction of the *miR-17-92* cluster into the MGC-803 cells significantly promoted cell growth due to the increased cellular proliferation and decreased cellular apoptosis, which were detected by CCK-8, cell viability and TUNEL assays. Moreover, the results of western blot analyses revealed that the activated protein kinase B (AKT), extracellular-signal-regulated kinase (ERK) and nuclear factor (NF-κB) signaling pathways were activated in these processes. Moreover, the overexpression of the *miR-17-92* cluster markedly enhanced the migratory and invasive abilities of the MGC-803 cells, which was associated with the occurrence of epithelial-mesenchymal transition (EMT). Tumor necrosis factor receptor associated factor 3 (TRAF3), which negatively regulates the NF-κB signaling pathway, was identified as a direct target of *miR-17-92*. Furthermore, TRAF3 silencing enhanced the oncogenic functions of the *miR-17-92* cluster in the MGC-803 cells, including the increased cellular proliferation, migration and invasion. Moreover, immunohistochemical staining and survival analyses of a gastric cancer tissue microarray revealed that TRAF3 functioned as a tumor suppressor in gastric cancer. Taken together, the findings of this study provide new insight into the specific biological functions of the *miR-17-92* cluster in gastric cancer progression by directly targeting *TRAF3*.

Introduction

Gastric cancer ranks fourth among the most common cancer types of cancer and is the third leading cause of cancer-related mortality worldwide (1). Recent advances in the diagnosis and treatment of the disease have increased the early detection and have decreased the mortality of patients with gastric cancer over the past decades; however, there are still an estimated 28,000 new cases of gastric cancer and 10,960 related deaths in the US in 2017 (2). Gastric cancer is difficult to cure primarily as the majority of patients present with advanced disease, and even a large number of patients who undergo surgical resection succumb to the disease due to recurrence. A variety of oncogenes and tumor suppressor genes are involved in the development of gastric cancer; however, the precise mechanisms underlying the progression of gastric cancer remain to be determined. Therefore, there is an urgent to identify more specific biomarkers for the early diagnosis of and therapy targets for gastric cancer.

MicroRNAs (miRNAs or miRs) are small non-coding RNAs (~22 nucleotides in length) that can regulate the expression of their target genes by binding to the complementary sites in the 3'-untranslated regions (3'-UTRs) of their targeting mRNAs and further regulate either translational repression or mRNA degradation (3,4). miRNAs have been reported to play important roles in cellular processes, such as cell differentiation, cell growth and proliferation, migration, apoptosis, metabolism and defense (5,6). Mounting evidence indicates that the aberrant expression of miRNAs or miRNA mutations are associated with diverse human malignancies, suggesting that miRNAs can function as tumor suppressors or oncogenes (7). miRNA expression profiles, determined using miRNA microarrays, reverse transcription-quantitative polymerase chain reaction (RT-qPCR) and next-generation sequencing (NGS) approaches, can be used to establish sample specificity and to identify cancer type (8). Tsai *et al* summarized a variety of

Correspondence to: Dr Weichang Chen, Department of Gastroenterology, The First Affiliated Hospital of Soochow University, 188 Shizi Road, Suzhou, Jiangsu 215006, P.R. China
E-mail: weichangchen@126.com

Dr Feng Guo, Department of Oncology, The Affiliated Suzhou Hospital of Nanjing Medical University, 16 Baita West Road, Suzhou, Jiangsu 215001, P.R. China
E-mail: guofeng27@suda.edu.cn

aberrantly expressed miRNAs as potential useful biomarkers for gastric cancer screening, diagnosis, prognosis, disease monitoring, as well as therapeutic targets (8). However, the exact role of specific miRNAs in regulating the tumorigenesis and progression of gastric cancer remains largely unknown.

The *miR-17-92* cluster, also known as *oncomiR-1*, is one of the most well-known oncogenic miRNAs (9). Human *miR-17-92* is located within intron 3 of the *C13orf25* gene at 13q31.3, and is frequently amplified in a variety of malignant tumors (10). The *miR-17-92* cluster has 6 mature miRNAs which are classified into 3 separate miRNAs families, including the *miR-17* family (*miR-17*, *miR-18* and *miR-20*), the *miR-19* family (*miR-19a* and *miR-19b*) and the *miR-92* family (*miR-92*). Previous studies have demonstrated that the expression of the *miR-17-92* cluster is upregulated in a variety of tumors originating from the lungs (11), breast (12), kidneys (13), liver (14), colon 15) and stomach (16). Generally, the *miR-17-92* cluster promotes tumorigenesis by negatively regulating tumor suppressors or genes, which are associated with a large variety of biological behaviors including cell proliferation, cell cycle, cell apoptosis, migration and metastasis (17).

The role of the *miR-17-92* cluster in gastric cancer is unclear. The majority of the published studies indicate that the *miR-17-92* cluster plays oncogenic roles in gastric cancer progression. In patients with gastric cancer, the levels of *miR-17-92* members in serum have been shown to be over-expressed, and are thus considered as potential biomarkers for the early detection of gastric cancer (16). Moreover, the *miR-17-92* cluster has been shown to be upregulated in gastric cancer tissues and serves as an independent prognostic marker in gastric cancer patients (18). *miR-92a* is used as a predictive prognostic marker in gastric cancer (19). Another study demonstrated that circulating *miR-18a* can be a useful biomarker for the screening of gastric cancer and monitoring cancer dynamics (20). The overexpression of *miR-17-5p* has been shown to increase the proliferation and growth of gastric cancer cells *in vitro* and *in vivo* by repressing *suppressors of cytokine signaling 6* (*SOCS6*) (21). The overexpression of miR-17 in gastric cancer cells is associated with certain proliferation-associated genes amplification, including *myelocytomatosis* (*MYC*), *cyclin E1* (*CCNE1*), *V-Erb-B2 avian erythroblastic leukemia viral oncogene homolog 2* (*ERBB2*) and *fibroblast growth factor receptor 2* (*FGFR2*) (22). miR-18a acts as an oncogene and plays an important role in gastric cancer by negatively regulating *protein inhibitor of activated signal transducer and activator of transcription 3* (*PIAS3*) (23). *miR-19a/b* has been shown to facilitate the migration and invasion of gastric cancer cells by targeting the antagonist of *c-myelocytomatosis-mitotic arrest deficient protein 1* (*c-Myc-MXD1*) (24). Moreover, *miR-19a/b* has been demonstrated to regulate multidrug resistance in gastric cancer cells by targeting *phosphate and tension homology deleted on chromsome ten* (*PTEN*) (25). *miR-19b*, *miR-20a* and *miR-92a* have been reported to play important roles in the development of gastric cancer stem cells (26). However, the critical role of the *miR-17-92* cluster in regulating gastric cancer progression remains unclear.

In this study, we systematically investigated the biological functions and the underlying mechanisms of action of the *miR-17-92* cluster in gastric cancer. The overexpression of the *miR-17-92* cluster in MGC-803 human gastric cancer cells affected a variety of biological functions, including cell growth, proliferation, apoptosis, migration and invasion. Activated protein kinase B (AKT), extracellular-signal-regulated kinase (ERK) and nuclear factor kappa-light-chain-enhancer of activated B cells (NF-κB) signaling pathways were involved in these processes. Importantly, for the first time, at least to the best of our knowledge, we identified that *tumor necrosis factor receptor associated factor 3* (*TRAF3*) was a direct and functional target of the *miR-17-92* cluster in MGC-803 gastric cancer cells. The loss-of-function of TRAF3 led to the acquirement of phenotypes, similar to what had been observed in the MGC-803 cells overexpressing the *miR-17-92* cluster. Survival analyses revealed that TRAF3 served as an important prognostic indicator in patients with gastric cancer. Herein, we demonstrate that the *miR-17-92* cluster functions as an onco-gene in gastric cancer by directly targeting *TRAF3*. Targeting the miR-17-92/TRAF3/NF-κB axis may thus prove to be a potent therapeutic approach in human gastric cancer.

Materials and methods

Cell culture. The human gastric cancer cell lines, AGS, SGC-7901, BGC-823, MKN-45 and MGC-803, were obtained from the Key Laboratory of Medicine and Clinical Immunology of Jiangsu Province, the First Affiliated Hospital of Soochow University. The 293T cells (provided by Professor Yong Zhao, Institute of Zoology, Chinese Academy of Sciences, Beijing, China) were maintained in our central laboratory. All the cells were cultured in RPMI-1640 medium supplemented with 10% fetal bovine serum (FBS), 100 U/ml penicillin, 100 μg/ml streptomycin and 2 mM glutamine. All the cells were cultured at 37˚C in a humidified atmosphere containing 5% CO_2.

Transfection. The *miR-17-92* cluster overexpression vector was constructed on the MSCV vector containing green fluorescent protein (GFP; from Professor Yong Zhao, Institute of Zoology, Chinese Academy of Sciences, Beijing, China). The MSCV-GFP-*miR-17-92* or MSCV-GFP control plasmid was transfected into the Phoenix A packaging cells (provided by Professor Yong Zhao, Institute of Zoology, Chinese Academy of Sciences) using FuGENE HD transfection reagent (cat. no. 04709705001; Roche, Shanghai, China). Viral supernatants were collected and used to infect the MGC-803 cells. For obtaining stably expressing cell lines, the cells were selected in the presence of 5 μg/ml puromycin (cat. no. J593; Amresco, Beijing, China). A shRNA-carrying sequence targeting the *TRAF3* gene (506-524: 5'-GATAAGGTGTTTAAGGATA-3') was designed and synthesized by Invitrogen (Beijing, China). The shRNA-TRAF3 was subcloned into the pSilencer3.1-H1-neo plasmid (cat no. 5770; Thermo Fisher Scientific™, Shanghai, China). The recombinant pSilencer3.1-siTRAF3 plasmid or the pSilencer3.1-H1-neo control plasmid were then trans-fected into the MGC-803 cells using Lipofectamine 2000 (cat no. 12566014; Thermo Scientific™). To obtain stably transfected cell lines, the cells were selected in the presence of 600 ng/μl neomycin (cat. no. A1720-5G; Sigma, Beijing, China).

RT-qPCR. Total RNA (2 μg) was reverse transcribed with SuperScript M-MLV (cat. no. 28025013; Promega, Shanghai,

China) according to the manufacturer's instructions. All RT-qPCR reactions were performed with a LightCycler 480 system (Roche) in triplicate. Primers were designed using Primer-BLAST (https://www.ncbi.nlm.nih.gov/tools/primer-blast/; NCBI; PubMed) and synthesized from Invitrogen (Beijing, China). *β-actin* was used as an internal control. cDNA was amplified using 2X LC480 SYBR-Green Master Mix (cat. no. 04887352001; Roche). Data were analyzed with the Pfaffl method (27,28). The primer sequences were as follows: *BIM* forward, 5'-ACAGAGCCACAAGACAGGAGCCC-3' and reverse, 5'-CGCCgGCAACTCTTGGGCGAT-3'; cyclin D1 (*CCND1*) forward, 5'-CACTTTCAGTCCAATAGGTGTAG-3' and reverse, 5'-TTCTTCTTGACTGGCACG-3'; *PTEN* forward, 5'-TGGGGAAGTAAGGACCAGAGA-3' and reverse, 5'-TGAGGATTGCAAGTTCCGCC-3'; Von Hippel-Lindau (*VHL*) forward, 5'-GCAGGCGTCGAAGAGTACG-3' and reverse, 5'-CGGACTGCGATTGCAGAAGA-3'; PH domain and leucine rich repeat protein phosphatase 2 (*PHLPP2*) forward, 5'-GTACGCAAGGGAAAGACCCA-3' and reverse, 5'-AGCAAGGGAGTATTGCCGTC-3'; *TRAF3* forward, 5'-TGTAAATACCGGGAAGCCACA-3' and reverse, 5'-TGCACTCAACTCGCTCCTCA-3'; *β-actin* reverse, 5'-GCTACGAGCTGCCTGACGG-3' and reverse, 5'-TGTTGGCGTACAGGTCTTTGC-3'.

RT-qPCR analysis of mature miRNA expression. Total RNA (2 μg) was polyadenylated with ATP by *E. coli* poly (A) polymerase (PAP; cat. no. M0276L; New England Biolabs, Ltd., Beijing, China). Following phenol-chloroform extraction and ethanol precipitation, the polyadenylated RNA was reverse transcribed with M-MLV and universal RT primer sequence. The cDNA (1:5 dilution) was then amplified using 2X LC480 SYBR-Green Master Mix (Roche). Each sample was determined in triplicate. *U6* expression was considered as an internal control. Data were analyzed using the Pfaffl method (27,29). The primer sequences were as follows: *hsa-miR-17* 5'-GCAAAGTGCTTACAGTGCAGGTAG-3'; *hsa-miR-18*, 5'-CCGGTAAGGTGCATCTAGT-3'; *hsa-miR-19a*, 5'-TGTGCAAATCTATGCAAAACTG-3'; *hsa-miR-19b*, 5'-GCATCCCAGTGTGCAAATCC-3'; *hsa-miR-20*, 5'-GGTAAAGTGCTTATAGTGCAGGTAG-3'; *hsa-miR-92*. 5'-ATTGCACTTGTCCCGGCCTGT-3'; *RT primer*, 5'-AACGAGACGACGACAGACTTTTTTTTTTTTTTV-3'; *U6*, 5'-GCAAATTCGTGAAGCGTTCCATA-3'.

Western blot analysis. Whole-cell extracts (WCE), cytoplasmic extracts (CE) and nuclear extracts (NE) were prepared using suspension buffer (10 mM Tris-HCl, 0.1 M NaCl, 1 mM EDTA) and proteinase inhibitor (cat. no. 11697498001; Roche Diagnostics, Mannheim, Germany) according to standard procedures. The total protein was measured with a micro BCA protein assay. Proteins (50 μg) were fractionated on an 10% SDS-PAGE gel and then transferred onto nitrocellulose membranes. After blocking with 5% milk in PBS for 1 h at room temperature, the membranes were incubated with primary antibodies (Abs). After washing, the membranes were incubated with secondary Abs. Finally, proteins were detected using the Odyssey system (LI-COR Biosciences, Lincoln, NE, USA). Abs (1:200 dilution) against RelA (sc-372X), RelB (sc-226X), c-Rel (sc-70), p105/p50 (sc-7178X), p100/p52 (sc-298), inhibitor of kappa B (IκB-α; sc-1643), p-IκB-α (Ser32/36, sc-101713),

cyclin D1 (sc-20044) and Lamin A/C (sc-20681) were purchased from Santa Cruz Biotechnology (Santa Cruz, CA, USA). Abs (1:1,000 dilution) against AKT (#4691), p-AKT (Ser473, #4060), p-AKT (Thr308, #2965), p-c-Raf (#9421), p-glycogen synthase kinase (GSK)-3β (#5558), p-PTEN (#9551), phosphorylated phosphoinositide-dependent protein kinase-1 (p-PDK1; #3438), ERK1/2 (#4695), p-ERK1/2 (#4370S), BIM (#2933), PTEN (#9559), VHL (#2738), TRAF3 (#4729), E-cadherin (#3195), claudin1 (#13255), epithelial cellular adhesion molecule (EpCAM; #14452), CK8/18 (#4546), N-cadherin (#13116) and Vimentin (#5741) were obtained from Cell Signaling Technology. Abs (1:1,000 dilution) against α-tubulin (AJ1034a) and β-actin (AO1215a) were purchased from Abgent (Suzhou, China). Secondary Abs (1:10,000 dilution) against IRDye 680CW (926-32222) and IRDye 800CW (926-32210) were obtained from LI-COR Biosciences (Lincoln, NE, USA).

NF-κB activity assay. NE preparation and TransAM assay were performed as previously described (30). The activity of individual NF-κB subunits was detected by an ELISA-based NF-κB family transcription factor assay kit (cat. no. 43296; Active Motif, Carlsbad, CA, USA). Briefly, nuclear extracts (2 μg) were incubated in a 96-well plate, which were immobilized NF-κB consensus oligonucleotides. The captured complexes were incubated with specific NF-κB primary Abs and subsequently detected with HRP-conjugated secondary Abs (included with the kit). Finally, the optical density (OD) value at 450 nm was measured by spectrophotometry (ELx800; BioTek Instruments, Winooski, VT, USA).

Cell proliferation assay (CCK-8). The cells were harvested and seeded in a 96-well plate at a density of 5×10^3 cells per well with 100 μl of complete culture medium, and incubated overnight at 37˚C in a 5% CO_2 humidified incubator. Cell growth rate was assessed using a cell counting kit-8 (cat. no. CK04; Dojindo, Kumamoto, Japan) at different time points (0, 24, 48 or 72 h). Briefly, CCK-8 (10 μl) was added to each well. Following incubation for 2 h at 37˚C, the absorbance at 450 nm was detected using a plate reader (ELx800; BioTek Instruments). Cell growth was measured by the relative absorbance with the absorbency of culture medium deducted.

Cell viability assay. The cells were harvested and seeded in a 96-well plate at a density of 5×10^3 cells per well with 100 μl of complete culture medium, and incubated overnight at 37˚C in a 5% CO_2 humidified incubator. Cell viability assay was performed using CellTiter-Glo (cat. no. G7570; Promega, Shanghai, China) according to the manufacturer's instructions. Briefly, CellTiter-Glo (100 μl) was added to each well. Following incubation for 10 min at room temperature, the luciferase activities were detected using a plate reader (ELx800; BioTek Instruments) CellTiter-Glo measurements were taken at individual time points (0, 24, 48 or 72 h) to track cell proliferation.

Terminal nucleotidyl transferase-mediated nick-end labeling (TUNEL) assay. The cells were cultured on cover slides for 24, 48 and 72 h at 37˚C overnight. TUNEL assay was performed according to the manufacturer's instructions of the TUNEL

system kit (Roche). In brief, the slides were fixed by 4% paraformaldehyde for 30 min and blocked with 3% H_2O_2 methanol solution for 10 min. The slides were then treated with 1% Triton PBS solution for 2 min. Subsequently, 50 μl of TUNEL reaction solution were added to incubate the cells on slides for 1 h at 37°C. Finally, the TUNEL signals were converted using peroxidase (POD) for 30 min at 37°C, and the sections were treated with DAB for 3 min. The results were observed under alight system microscope IX71 (Olympus, Tokyo, Japan).

Scratch wound healing assay. For the scratch healing assays, THE cells were treated with 10 mg/ml mitomycin C (Sigma, Beijing, China) for 3 h. Subsequently, the cells were wounded using a 200 μl sterile pipette tip, washed 3 times with PBS, and RPMI-1640 with 10% FBS was added. The wound closure was imaged continuously for 24, 48 and 72 h under a magnification of x10 using the light System Microscope IX71 (Olympus).

Transwell migration and invasion assay. Transwell chambers (cat. no. 3422, 8 μm, 24-well insert; Corning, Lowell, MA, USA) were used for the migration and invasion assay. In brief, 600 μl of 10% FBS-containing medium was added to the lower chamber and $1x10^5$ cells in 200 μl serum-free medium were added to the upper chamber. The cells were incubated for 24 h at 37°C, and the non-invading cells were removed. Finally, the insert membranes were fixed with 4% paraformaldehyde, stained with 0.1% crystal violet (C8470; Solarbio, Beijing, China) for 15 min at room temperature, and photographed under an inverted microscope (SystemMicroscope IX71; Olympus, Tokyo, Japan). For the invasion assay, the insert membranes were coated with diluted Matrigel (cat. no. 354234; BD Biosciences, San Jose, CA, USA). Subsequently, $1x10^5$ cells were added to the upper chamber. At least 3 randomly selected fields were observed, and the average cell number was calculated.

Gelatinase zymography assay. For the gelatinase zymography assay, the activities of matrix metalloproteinase (MMP)-9 and -2 were examined. Culture medium was loaded on an 8% SDS-PAGE gel in the presence of 0.1% gelatin under non-reducing conditions. Culture medium samples were not denatured prior to electrophoresis. Following electrophoresis, the gels were washed twice in 2.5% Triton X-100 for 30 min. The gels were then incubated in substrate buffer (50 mM Tris-HCl and 10 mM $CaCl_2$, pH 8.0) at 37°C overnight, and stained with 0.5% Coomassie blue R250 (50% methanol and 10% glacial acetic acid) for 30 min, and then de-stained. Upon renaturation of the enzyme, the gelatinases digested the gelatin in the gel to produce clear bands against an intensely stained background.

Luciferase reporter assay. The 3'-untranslated region (UTR) of *TRAF3* mRNA was amplified by PCR from genomic DNA of the MGC-803 human gastric cancer cell line and ligated into the pmirGLO dual-luciferase miRNA target expression vector (#E1330; Promega, Madison, WI, USA). The primer sequences of the 3'-UTR of *TRAF3* mRNA were as follows: 5'-CTGGACATGTCAGCATGTTAAGT-3' and 5'-CGAGGCTCCGTTCAGAATTG-3'. The mutant constructs were generated using a Site-Directed Mutagenesis kit

(#SDM-15, Beijing SBS Genetech Co., Ltd., Beijing, China). The 293T cells were seeded in 24-well plates at a density of $5x10^4$ cells per well with 500 μl of complete culture medium, and incubated overnight at 37°C in a 5% CO_2 humidified incubator. The pmirGLO-TRAF3-3'-UTR-wt plasmid or pmirGLO-TRAF3-3'-UTR-mut plasmid was co-transfected into the 293T cells with the *miR-17-92* plasmid or control plasmid using Lipofectamine 2000 reagent (#11668-027; Invitrogen/Thermo Fisher Scientific, Waltham, MA, USA), respectively. Luciferase and *Renilla* activities were evaluated 48 h following transfection using the Dual-GLO® Luciferase Assay System (#E2920; Promega, Madison, WI, USA) according to the manufacturer's instructions.

In vivo tumorigenesis. Four-week-old male BALB/c-nude mice were purchased from Shanghai Slac Laboratory Animal Co. Ltd., Shanghai, China. The animals were randomly classified into 2 groups as follows: the MGC-803-control group and the MGC-803-miR-17-92 group, and each group had 5 mice. A total of $5x10^6$ cells were resuspended in 200 μl PBS and then injected subcutaneously into the right flanks of the nude mice. Tumor volume was measured every 4 days using a digital caliper according to the following formula: TV (mm^3) = 0.5 x length x $width^2$. All the mice were sacrificed at 32 days after the injection. The tumors were excised, photographed, measured, weighted and fixed in 10% neutralized formalin overnight. The tumor tissues were dehydrated, fixed in paraffin, and cut into 5-μm-thick sections for histopathological examination and immunohistochemistry (IHC). The sections were stained for TRAF3 (dilution 1:50) expression using standard protocols. The sections were developed with 3,3-diaminobenzine (DAB) and counterstained with hematoxylin. All procedures and animal experiments were approved by the Animal Care and Use Committee of Soochow University.

Clinical samples. The commercial human gastric cancer tissue microarray was purchased from Shanghai Outdo Biotech Company from the National Human Genetic Resources Sharing Service Platform (2005DKA21300). It consists of 100 paired gastric cancer and adjacent normal tissues, and was used to evaluate the protein expression of TRAF3. Patient follow-up information was obtained from 2007 to 2014. The information was obtained from the microarray company.

IHC. The IHC assay of tissue microarray was performed using a standard peroxidase-based staining method. Tissue sections (5-μm-thick) were incubated in a dry oven at 60°C for 30 min and then deparaffinized in xylene for 10 min in triplicate, rehydrated with graded ethanol in 100, 95, 90, 80 and 70% ethanol for 5 min each. Antigen retrieval was then performed using 0.01 M citrate buffer (pH 6.0). Subsequently, the slides were treated with 3% hydrogen peroxide (H_2O_2) to block endogenous peroxidase. The slides were then blocked with 5% bovine serum albumin (BSA; Boster Bioengineering, Wuhan, China), incubated with mouse anti-TRAF3 antibody (#4729; Cell Signaling Technology, 1:50 dilution) overnight at 4°C. Subsequently, the slides were incubated with diluted secondary antibody (#7076; Cell Signaling Technology, 1:500 dilution) for 45 min at 37°C. Finally, the slides were treated with DAB and counterstained
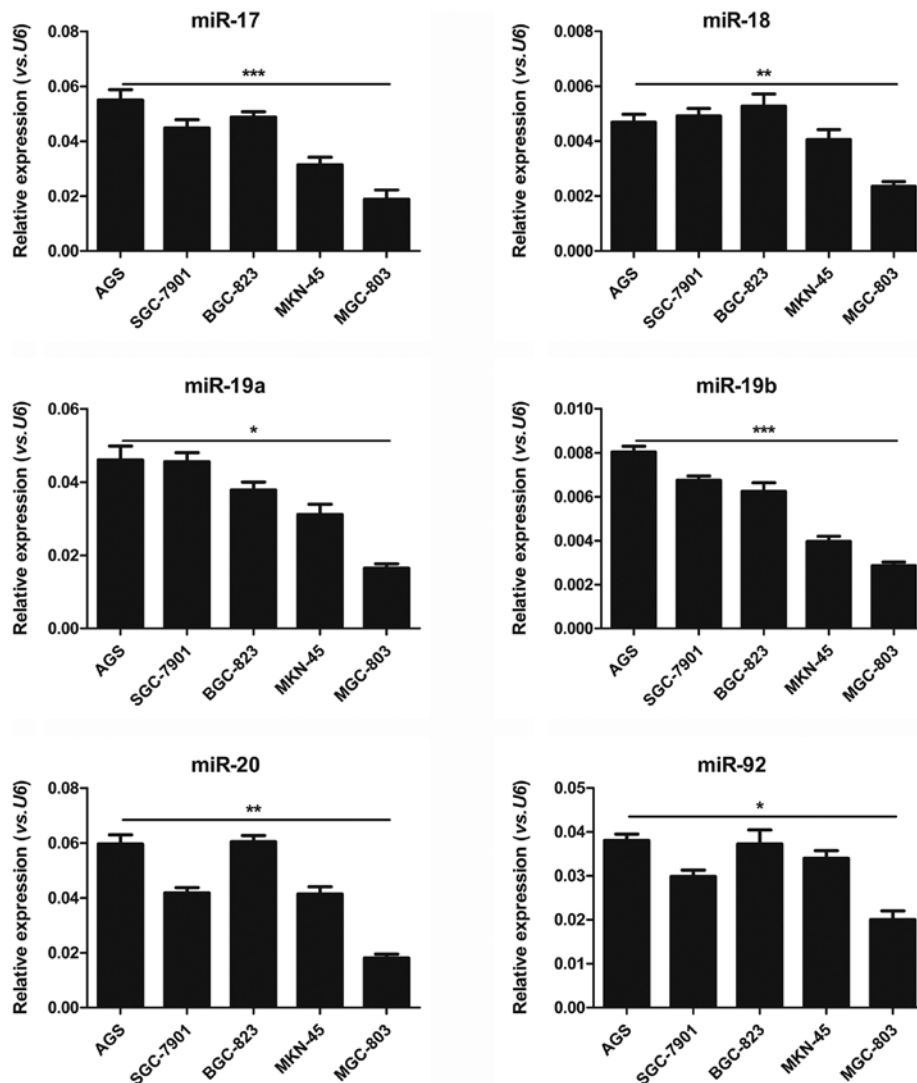
Figure 1. Distinct *miR-17-92* expression patterns in human gastric cancer cell lines. RT-qPCR analysis of the expression of the 6 *miR-17-92* family members (*miR-17*, *miR-18*, *miR-19a*, *miR-19b*, *miR-20* and *miR-92*) in AGS, SGC-7901, BGC-823, MKN-45 and MGC-803 human gastric cancer cell lines. Gene expression was normalized to *U6*, and measured in triplicate (Student's t-test, *P<0.05, **P<0.01, ***P<0.001).

with hematoxylin for microscopic examination. The results were observed by 2 independent investigators under an Olympus microscope BX 51 (Olympus) and scored as follows: 0, No staining; 1+, light; 2+, moderate; 3+, strong, according to the intensity of the staining. The percentage of positively stained cells was scored as follows: 0, No staining; 1, <25% staining; 2, 26-50% staining; 3, 51-75% staining; and 4, >75% staining. The product of the intensity and extent grades ≥4 of positive cells was considered high expression, and the score of 0-3 of positive cells was regarded as low expression.

Statistical analysis. All the experiments were repeated at least 3 times. All quantitative data are presented as the means ± SD and analyzed using the Student's t-test. The association between TRAF3 expression and the clinicopathological factors was estimated using the Chi-square test. Overall survival (OS) curves were plotted on the basis of the Kaplan-Meier method and analyzed using the log-rank test. All statistical analyses were performed using GraphPad Prism version 5.0. A P-value ≤0.05 was considered to indicate a statistically significant difference,

and P-values ≤0.01 and ≤0.001 were considered to indicate highly significant differences.

Results

Distinct miR-17-92 expression patterns in human gastric cancer cell lines. The expression of the *miR-17-92* cluster, including *miR-17*, *miR-18*, *miR-19a*, *miR-19b*, *miR-20* and *miR-92*, was detected by RT-qPCR analyses of human gastric cancer cell lines, including AGS, SGC-7901, BGC-823, MKN-45 and MGC-803. As shown in Fig. 1, all of the 6 members of the *miR-17-92* cluster could be clearly detected in individual human gastric cancer cell lines, albeit with different levels. The expression levels of the individual *miR-17-92* members in the AGS cells were comparable to those in the SGC-7901 and BGC-823 cells. However, the expression levels of the *miR-17-92* cluster in the MKN-45 and MGC-803 cells were significantly lower than those in the AGS, SGC-7901 and BGC-823 cells. The expression levels of *miR-17* (P=0.0003), *miR-18* (P=0.0041), *miR-19a* (P=0.0114), *miR-19b* (P=0.0008), *miR-20* (P=0.0086) and *miR-92* (P=0.0348) were significantly
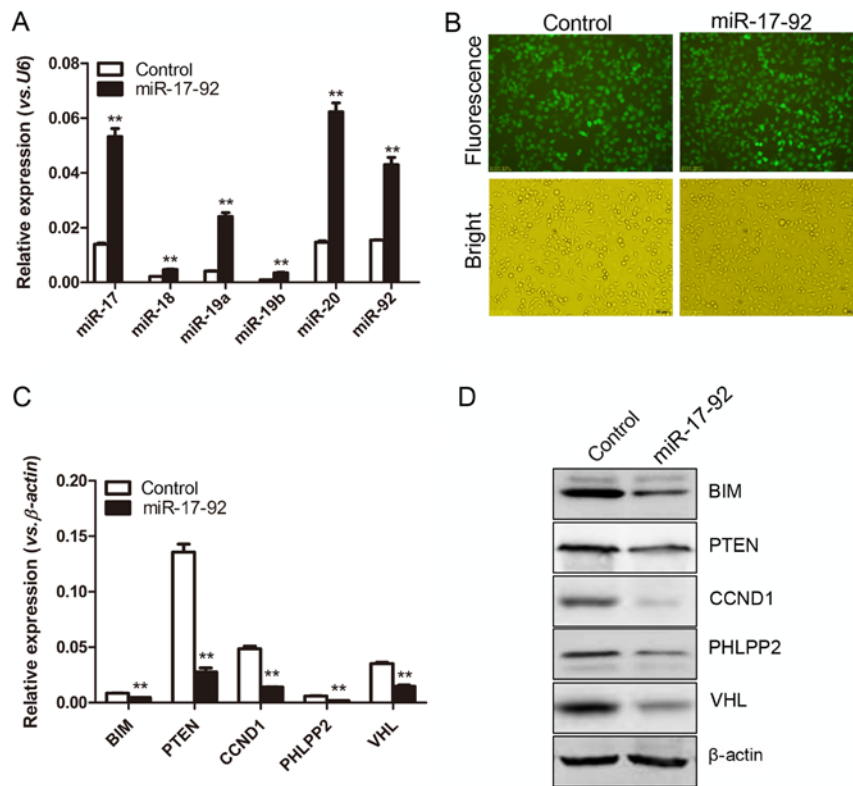
Figure 2. Establishment of a miR-17-92-overexpressing MGC-803 cell line. (A) The expression of the individual *miR-17-92* family members in the established MGC-803-control and MGC-803-miR-17-92 cell lines was analyzed by RT-qPCR. Gene expression was normalized to *U6*, and measured in triplicate. Significant differences are indicated (Student's t-test, **P<0.01). (B) Representative images of GFP signals between the 2 established cell lines. GFP signals in MGC-803-control and MGC-803-miR-17-92 cells were observed under a fluorescence microscope. The upper 2 images, show an original magnification of x40, under a fluorescent field, while the lower 2 images show the bright field. (C) mRNA levels of target genes of the *miR-17-92* cluster were determined by RT-qPCR analysis. Gene expression was normalized to *β-actin*, and measured in triplicate. Significant differences are indicated (Student's t-test, **P<0.01). (D) Protein levels of target genes of the *miR-17-92* cluster were determined by western blot analysis. The level of each protein was normalized to β-actin.

decreased approximately 2- to 4-fold in the MGC-803 cells, as compared with those in the AGS cells. It was indicated that the *miR-17-92* expression levels in the MGC-803 cells were the lowest among the 5 human gastric cancer cell lines. Thus, the MGC-803 cell line was selected to perform the following experiments to explore the function of the *miR-17-92* cluster in gastric cancer progression.

Establishment of a miR-17-92-overexpressing MGC-803 cell line. To explore the effects of the *miR-17-92* cluster on the biological behaviors of the MGC-803 cells, the constructed *miR-17-92* overexpression plasmid was transfected into the MGC-803 cells. The positive monoclones were selected upon exposure to puromycin (5 ng/µl) for 2 weeks. The formed monoclones were further verified for *miR-17-92* expression by RT-qPCR analyses. The expression levels of each *miR-17-92* family member were significantly increased in the MGC-803-miR-17-92 cells compared to those in the MGC-803-control cells, 4-fold for *miR-17* (P=0.0109), 3-fold for *miR-18* (P=0.0415), 6-fold for *miR-19a* (P=0.0111), 5-fold for *miR-19b* (P=0.0104), 4-fold for *miR-20* (P=0.0058) and 2-fold for *miR-92* (P=0.0169), indicating a successful introduction of the *miR-17-92* cluster into the MGC-803 cells (Fig. 2A). Moreover, GFP was used as a marker for the transfection of the plasmids. As shown in Fig. 2B, both the established MGC-803-miR-17-92 and the MGC-803-control cells presented strong GFP signals observed under a

fluorescence microscope (Fig. 2B). The GFP signals of the MGC-803-miR-17-92 and the MGC-803-control cells were measured by flow cytometry. The percentages of GFP-positive cells in the 2 established cell lines were 95.71 and 96.88%, respectively (data not shown), indicating the successful transfection of the plasmids. Moreover, the expression levels of certain well-known target genes of the *miR-17-92* cluster, including *BIM*, *PTEN*, *CCND1*, *PHLPP2* and *VHL* were significantly decreased in the MGC-803-miR-17-92 cells compared to those in the MGC-803-control cells (Fig. 2C). Consistently, the expression levels of BIM, PTEN, cyclin D1, PHLPP2 and VHL at the protein level were decreased, as detected by western blot analysis (Fig. 2D). Taken together, it was indicated that the MGC-803 gastric cancer cell line stably overexpressing the *miR-17-92* cluster was successfully established.

miR-17-92 overexpression promotes proliferation and reduces apoptosis in vitro and accelerates tumor xenograft growth in vivo. To determine whether the overexpression of the *miR-17-92* cluster modulates the proliferative activity of the MGC-803 cells, a CCK-8 assay was performed. As shown in Fig. 3A, the OD values at 450 nm in the *miR-17-92* overexpression group (0.76±0.10 and 1.26±0.11) were significantly higher than those in the control group (0.37±0.06 and 0.61±0.08) at 48 and 72 h, respectively (both P<0.01). To further characterize the effects of *miR-17-92* on the viability
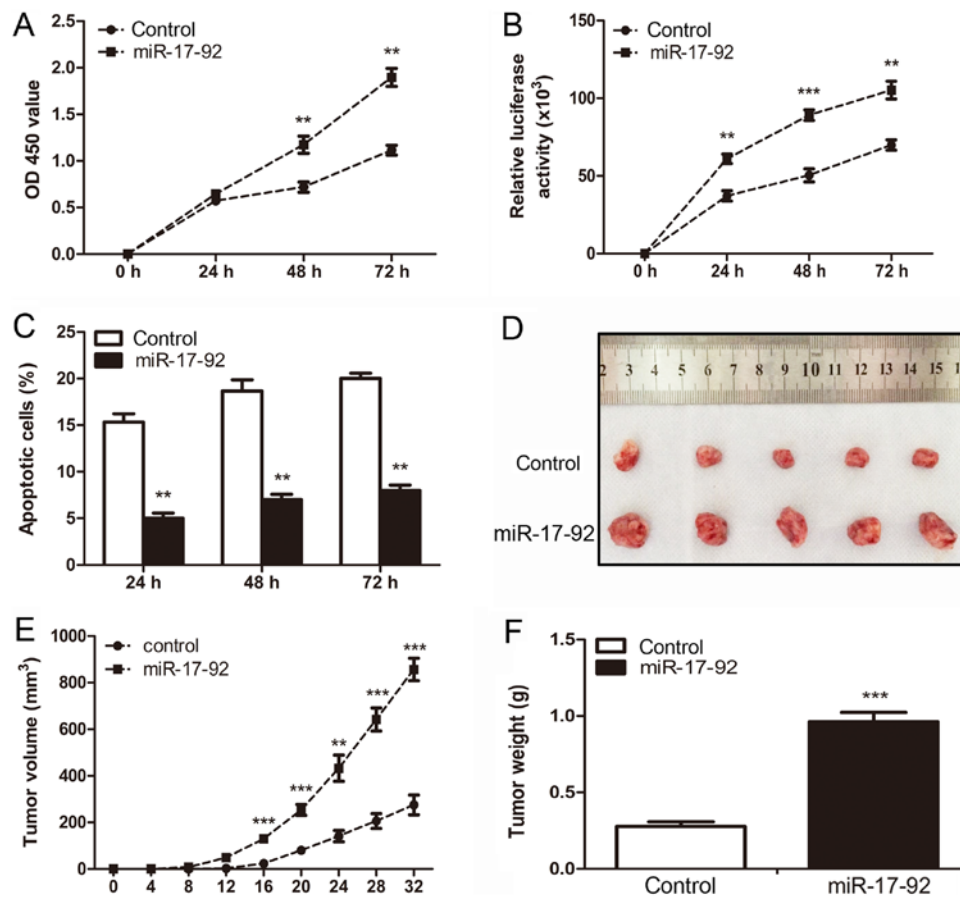
Figure 3. *miR-17-92* overexpression promotes proliferation and reduces apoptosis *in vitro* and accelerates xenograft tumor growth *in vivo*. (A) Cell proliferation activity between the MGC-803-control and MGC-803-miR-17-92 cells was analyzed by CCK-8 assay at 24, 48 and 72 h (Student's t-test, **P<0.01). (B) Cell viability assay was carried out to detect the viability of the 2 established cell lines at 24, 48 and 72 h. The relative luciferase activity was detected among the 2 established cell lines. Significant differences are indicated (Student's t-test, **P<0.01, ***P<0.001). (C) TUNEL assay was carried out to quantitatively evaluate the apoptotic cells between the 2 established cell lines at 24, 48 and 72 h. Significant differences are indicated (Student's t-test, **P<0.01). (D) Representative images of tumor growth in the mouse xenograft model. The MGC-803-control or MGC-803-miR-17-92 cells were injected subcutaneously into nude mice. Each group had 5 nude mice. (E) At 32 days after the injection, the mice were sacrificed and tumor volume was measured every 4 days after inoculation. Significant differences are indicated (Student's t-test, **P<0.01, ***P<0.001). (F) Tumors in individual mice were weighed. Significant differences are indicated (Student's t-test, ***P<0.001).

of the MGC-803 cells, a CellTiter-Glo cell viability assay was carried out. It was shown that the luciferase activities of the MGC-803-control cells were 37,098±6,833, 45,846±7,009 and 63,883±8,471 at 24, 48 and 72 h, respectively; while those in the MGC-803-miR-17-92 cells were 54,545±8,151, 86,085±5,774 and 102,027±11,564 (**P<0.01, ***P<0.001, Fig. 3B). To investigate whether the overexpression of *miR-17-92* affected the apoptotic capability of the MGC-803 cells, a TUNEL assay was performed. As shown in Fig. 3C, both the MGC-803-control and MGC-803-miR-17-92 cells underwent apoptosis in a time-dependent manner. The apoptotic rates of the MGC-803-control cells were 14.67±1.28, 18.28±1.75 and 20.17±1.76%, while those of the MGC-803-miR-17-92 cells were 5.33±1.28, 7.11±1.07 and 7.97±1.25% at 24, 48 and 72 h, respectively (all P<0.01). Moreover, the cell cycle was analyzed by flow cytometry, and the results revealed no significant differences between the MGC-803-control and MGC-803-miR-17-92 cells (data not shown).

To further investigate whether miR-17-92 overexpression can promote cell growth in vivo, BALB/c-nude mice were injected subcutaneously into the right flanks with the MGC-803-control or MGC-803-miR-17-92 cells to establish

a heterotopic xenograft tumor mouse model. A representative image of tumors from both the control and the *miR-17-92* overexpression group is shown in Fig. 3D. The mean tumor volume in the *miR-17-92* overexpression group reached >800 mm3, but was <400 mm^3 in the control group at 32 days following implantation (Fig. 3E). The mean tumor weight in the *miR-17-92* overexpression group (0.94±0.16 g) was much greater than that in the control group (0.26±0.08 g, P<0.001, Fig. 3F). Taken together, these results indicated that *miR-17-92* overexpression in the MGC-803 cells increased the proliferative activity and decreased the apoptosis of the gastric cancer cells *in vitro*, and promoted tumor xenograft growth *in vivo*.

miR-17-92 overexpression modulates the AKT, ERK and NF-kB signaling pathways. As shown in Fig. 4A, the protein expression of AKT signaling molecules, including AKT, p-AKT-473, p-AKT-308, p-c-Raf, p-GSK-3β, p-PTEN and p-PDK1, were measured by western blot analyses. Total AKT expression was similar between the MGC-803-control and MGC-803-miR-17-92 cells. However, *miR-17-92* over-expression induced the phosphorylation of AKT at Thr308, but not at Ser473 (Fig. 4A), which was due to the inhibition
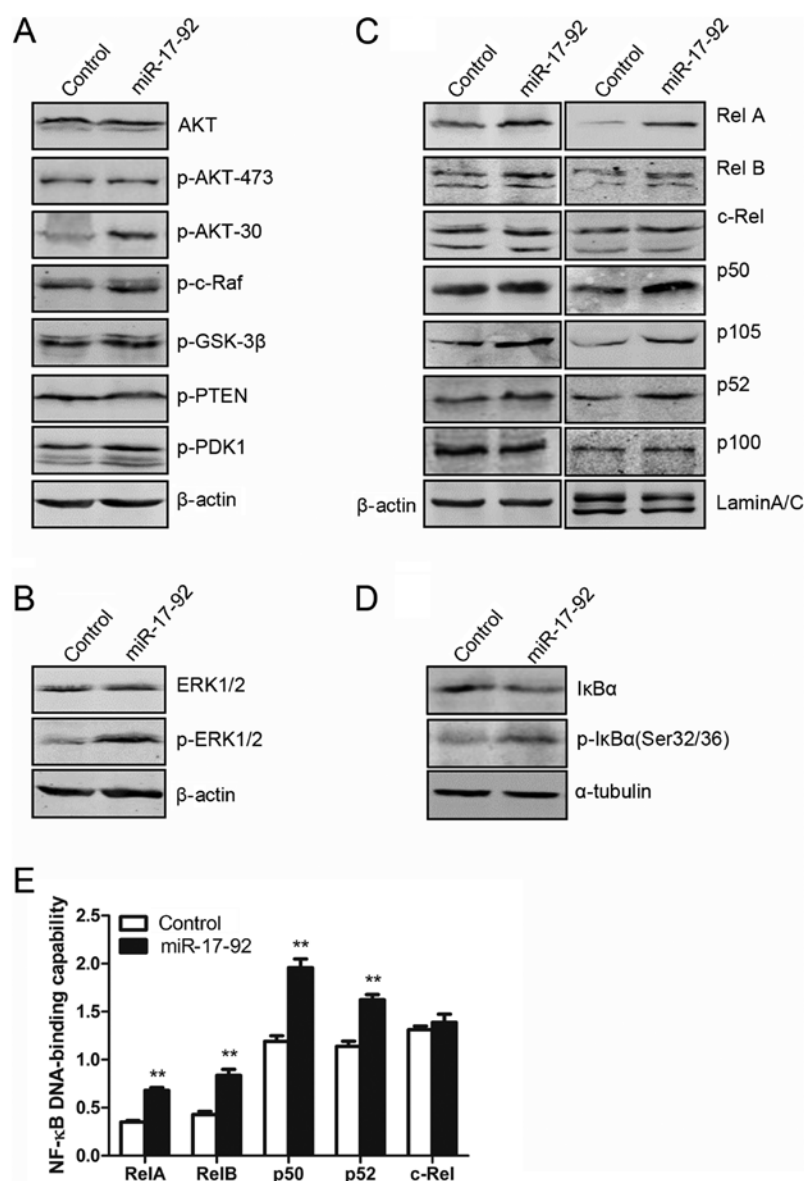
Figure 4. *miR-17-92* overexpression modulates the AKT, ERK and NF-κB signaling pathways. (A) The protein expression level of the AKT signaling pathway, including AKT, p-AKT (Ser473), p-AKT (Thr308), p-c-Raf, p-GSK-3β, p-PTEN and p-PDK1 examined by western blot analysis. The level of each protein was normalized to β-actin. (B) The protein expression of total ERK1/2 and p-ERK1/2 was examined by western blot analysis. The level of each protein was normalized to β-actin. (C) The protein expression of NF-κB subunits was examined by western blot analysis. Protein expression in cytoplasmic (CE) and nuclear portion (NE) was normalized to β-actin and LaminA/C, respectively. (D) The protein expression of IKB-α and p-IKB-α (Ser32/36) was examined by western blot analysis. The level of each protein was normalized to α-tubulin. (E) Nuclear extracts of cells were prepared and tested for the DNA-binding activities using the TransAM™ NF-κB family transcription factor assay kit (Student's t-test, **P<0.01).

of PTEN expression (Fig. 2D). No significant changes were observed in the other AKT signaling molecules (Fig. 4A). As shown in Fig. 4B, the protein expression level of total ERK1/2 in the MGC-803-miR-17-92 cells was comparable to that in the MGC-803-control cells. However, the overexpression of the *miR-17-92* cluster in the MGC-803 cells induced the phosphorylation of ERK1/2 (p-ERK1/2). Thus, *miR-17-92* overexpression in the MGC-803 cells induced p-ERK1/2 expression without affecting total ERK1/2 expression.

Subsequently, to investigate whether *miR-17-92* over-expression affects the activity of NF-κB signaling, western blot analysis was performed. As shown in Fig. 4C, the expression of RelA/p65 and p50, representing canonical NF-κB activity, was clearly increased in both the CE and NE fractions in the MGC-803-miR-17-92 cells compared to those in the MGC-803-control cells. The phosphorylation of IκB-α at Ser32/36 was induced by *miR-17-92* overexpression in the MGC-803 cells (Fig. 4D), leading to the subsequent degradation of IκB-α. The expression of IκB-α, an impor-tant upstream regulator of the canonical NF-κB signaling, was markedly decreased in the MGC-803-miR-17-92 cells. Moreover, the expression of RelB and p52, representing non-canonical NF-κB activity, was slightly increased in the NE of the MGC-803-miR-17-92 cells. However, the expres-sion of c-Rel in the MGC-803-miR-17-92 cells was similar to that in the MGC-803-control cells (Fig. 4C). To determine the exact contribution of the *miR-17-92* gene cluster to the NF-κB DNA-binding capabilities in the MGC-803 cells, an ELISA-based NF-κB activity assay was performed. As shown in Fig. 4E, the DNA-binding capability of each NF-κB
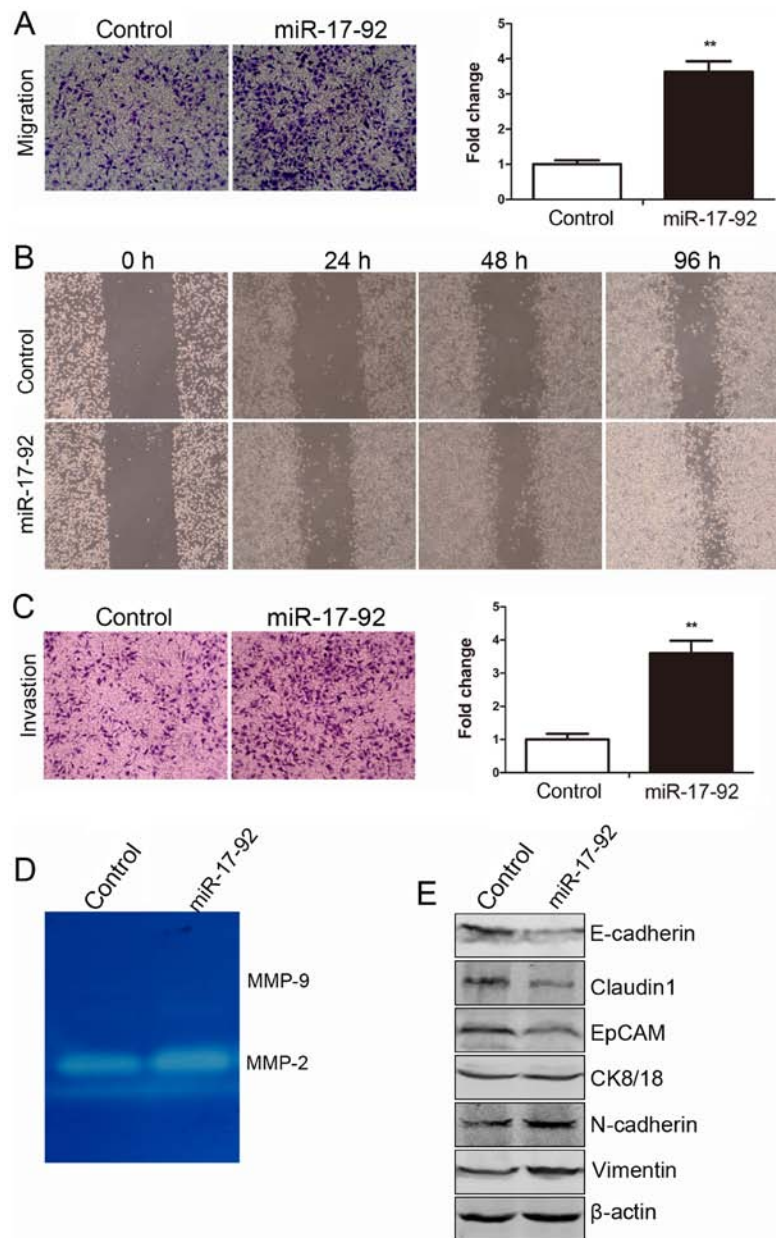
Figure 5. *miR-17-92* overexpression enhances the migratory and invasive abilities of the MGC-803 cells by regulating epithelial-mesenchymal transition (EMT). (A) The migratory ability of the MGC-803-control and MGC-803-miR-17-92 cells was detected by Transwell migration assay. Left panel, representative images of migrated cells between the 2 established cell lines were photographed under an inverted microscope (x20 magnification). Right panel, the number of migrated cells was quantified (Student's t-test, **P<0.01). (B) The migratory ability of the cells was detected by a scratch wound healing assay at 24, 48 and 72 h. (C) The invasive ability of the MGC-803-control and MGC-803-miR-17-92 cells was detected by Transwell invasion assay. Left panel, representative images of invaded cells between the 2 established cell lines were photographed under an inverted microscope (x20 magnification). Right panel, the number of invaded cells was quantified (Student's t-test, **P<0.01). (D) The activity of matrix metalloproteinase (MMP)-2 and MMP-9 was evaluated by the gelatin zymography assay. (E) The protein expression levels of E-cadherin, claudin1, EpCAM, CK8/18, N-cadherin and Vimentin were examined by western blot analysis in the 2 established cell lines. The level of each protein was normalized against β-actin.

subunit including RelA, p50, RelB and p52 in the NE of the MGC-803-miR-17-92 cells was significantly increased as compared with that in the MGC-803-control cells. However, the DNA-binding capability of c-Rel was comparable between the 2 cell lines. Taken together, these results indicated that the introduction of the *miR-17-92* cluster into the MGC-803 cells activated the AKT, ERK and NF-κB signaling pathways, likely contributing to the increased cellular proliferation.

miR-17-92 overexpression enhances the migratory and invasive abilities of the MGC-803 cells by regulating

epithelial-mesenchymal transition (EMT). As shown in Fig. 5A, the number of migrated cells in the *miR-17-92* overexpression group was increased approximately 3-fold as compared with that of the control group (P<0.01). Cell motility was also evaluated by scratch wound healing assay. As shown in Fig. 5B, a scratched cell monolayer was formed and images were captured at 24, 48 and 72 h. It was shown that the MGC-803-miR-17-92 cells migrated from the edge towards the scratch center more rapidly than the MGC-803-control cells, indicating an enhanced migratory ability. Transwell invasion assay was performed to further
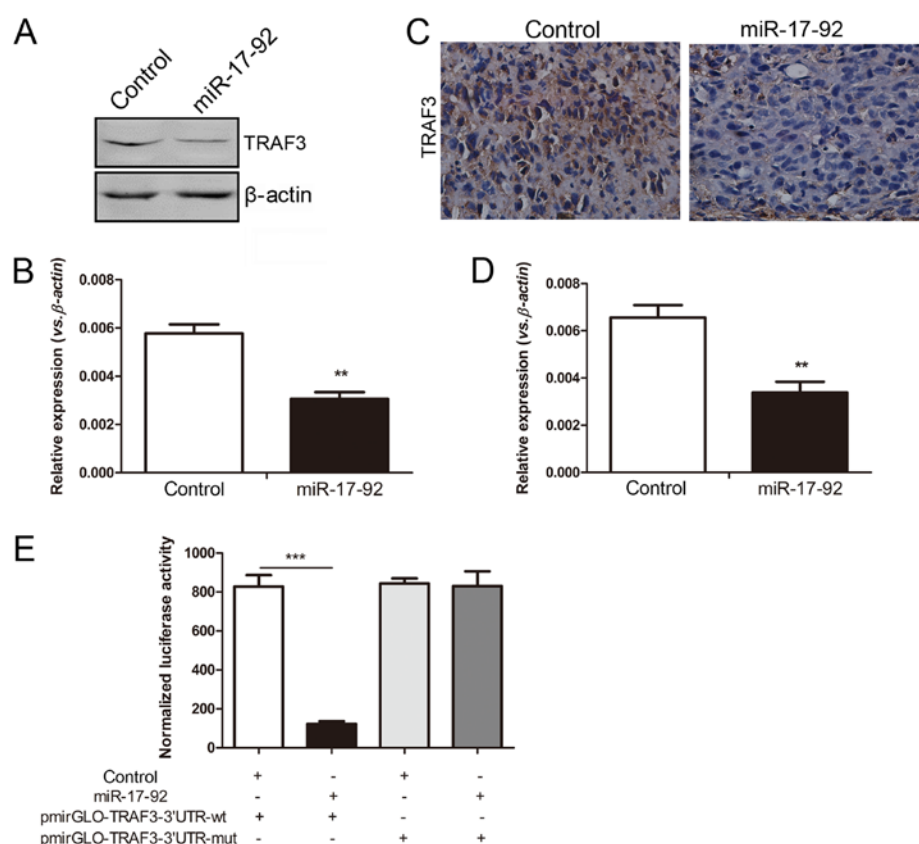
Figure 6. TRAF3 is a direct target of the *miR-17-92* cluster in the MGC-803 cells. (A) The protein expression of tumor necrosis factor receptor associated factor 3 (TRAF3) in the MGC-803-control and MGC-803-miR-17-92 cells was determined by western blot analysis. The level of each protein was normalized against β-actin. (B) The mRNA expression of *TRAF3* between the 2 established cell lines was determined by RT-qPCR analysis. Gene expression was normalized to *β-actin*, and measured in triplicate. Significant differences are indicated (Student's t-test, **P<0.01). (C) Representative images of TRAF3 protein expression levels in the tumor xenografts between the MGC-803-control and MGC-803-miR-17-92 groups were determined by immunohistochemistry and photographed under an inverted microscope (x40 magnification). (D) *TRAF3* mRNA expression levels between the 2 groups were determined by RT-qPCR analysis. Gene expression was normalized to *β-actin*, and measured in triplicate. Significant differences are indicated (Student's t-test, **P<0.01). (E) Luciferase reporter assay was performed after the 293T cells were transfected with luciferase vectors containing wide-type or mutant TRAF3-3'UTR and the control or *miR-17-92* plasmids, respectively. The luciferase activity was normalized to *Renilla* luciferase activity. Each group was allocated 6 wells. Significant differences are indicated (Student's t-test, ***P<0.001).

examine the role of *miR-17-92* in the invasive ability of the MGC-803 cells. As shown in Fig. 5C, the number of cells that invaded the Matrigel layer from the MGC-803-miR-17-92 group was increased approximately 4-fold compared with that of the MGC-803-control group (P<0.01). The results of the gelatin zymography assay revealed that MMP-9 activity was not detected in either of the established cell lines; however, MMP-2 activity was markedly increased in the MGC-803-miR-17-92 cells (Fig. 5D). The expression levels of key molecules involved in EMT, including E-cadherin, claudin1, EpCAM, CK8/18, N-cadherin and Vimentin, were examined by western blot analysis. The expression levels of claudin1 and EpCAM, representing epithelial markers, were decreased in the MGC-803-miR-17-92 cells compared to the MGC-803-control cells, while the expression levels of other epithelial markers, such as E-cadherin and CK8/18 were unaffected. The expression levels of N-cadherin and Vimentin, mesenchymal markers, were increased in the MGC-803-miR-17-92 cells compared with the MGC-803-control cells (Fig. 5E). Thus, EMT occurred when the *miR-17-92* cluster was overexpressed in the MGC-803 cells. Collectively, these results indicated that the enforced introduction of the *miR-17-92* cluster into the MGC-803 cells

enhanced the migratory and invasive abilities of the cells, which was owing to the occurrence of EMT.

TRAF3 is a direct target of the miR-17-92 cluster in the MGC-803 cells. Of note, we focused on the TRAF3 gene, as it was found to be one of the predicted target genes of the *miR-17-92* cluster using TargetScan Release 5.1 online software (http://www.targetscan.org/, Whitehead Institute for Biomedical Research, Cambridge, MA, USA) (data not shown). The protein expression of TRAF3 was significantly decreased in the MGC-803 cells overexpressing the *miR-17-92* cluster, which was in line with the decreased mRNA level detected by RT-qPCR analysis (Fig. 6A and B). The deregulated NF-κB family members were observed in the cells overexpressing the *miR-17-92* cluster. Compared with the control group, both the mRNA and protein expression levels of TRAF3 were decreased in the xenograft tumors in the *miR-17-92* overexpression group (Fig. 6C and D), which was consistent with the *in vitro* results.

To verify whether *TRAF3* is truly a direct target of the *miR-17-92* cluster, a luciferase assay was performed. The pmirGLO-TRAF3-3'-UTR-wild-type or pmirGLO-TRAF3-3'-UTR-mutant vector were co-transfected into 293T cells
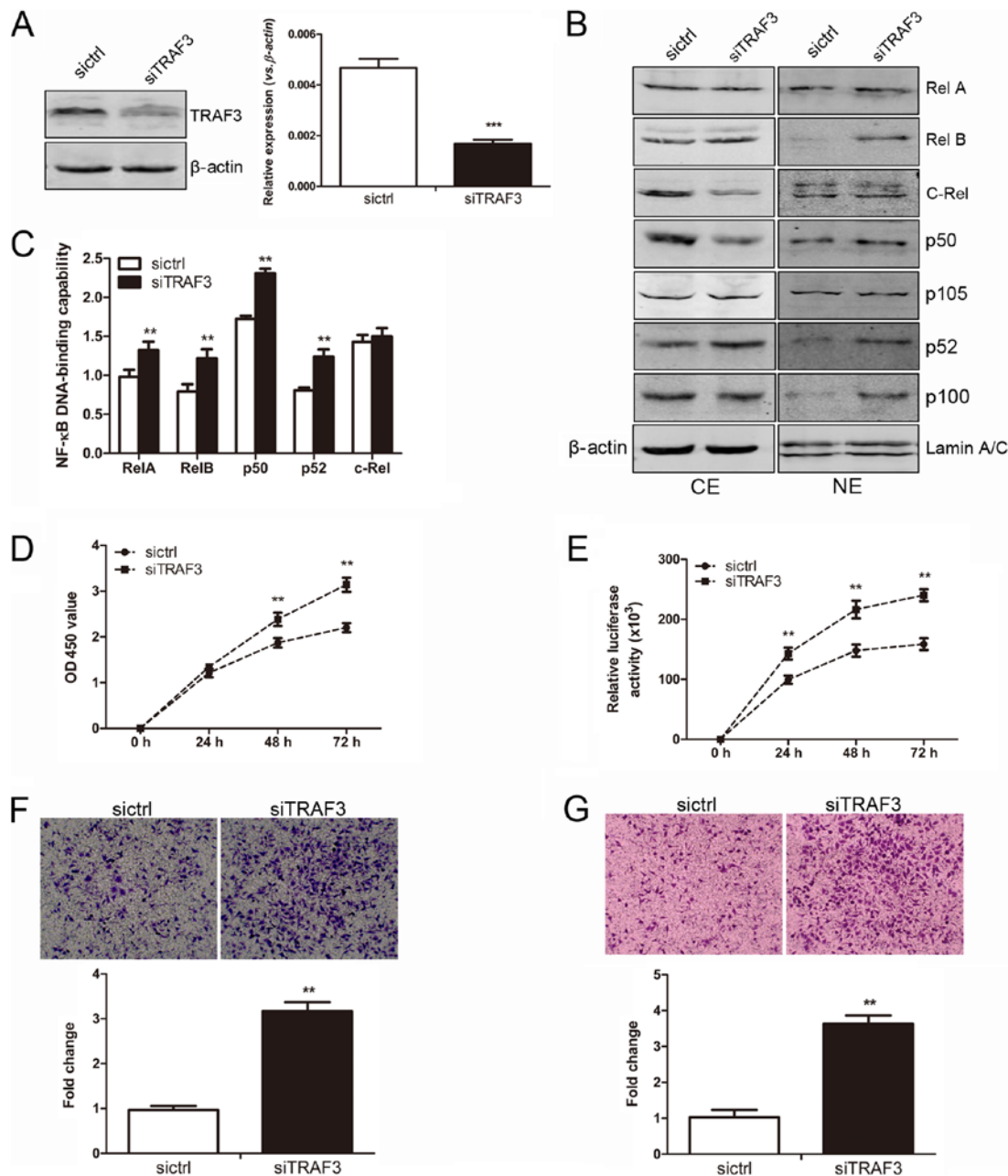
Figure 7. Tumor necrosis factor receptor associated factor 3 (*TRAF3*) silencing promotes cellular proliferation and enhances the migratory and invasive abilities of the MGC-803 cells *in vitro*. (A) The expression of TRAF3 was downregulated in the MGC-803 cells in which *TRAF3* was silenced. Left panel, the protein expression of TRAF3 in the MGC-803-sictrl and MGC-803-siTRAF3 cells was determined by western blot analysis. The level of each protein was normalized against β-actin. Right panel, the mRNA expression of *TRAF3* between the 2 established cell lines was determined by RT-qPCR analysis Gene expression was normalized to *β-actin*, and measured in triplicate. Significant differences are indicated (Student's t-test, ***P<0.001). (B) The protein expression of nuclear factor (NF)-κB subunits between the 2 established cell lines was examined by western blot analysis. Protein expression in the cytoplasmic extract (CE) and nuclear extract (NE) was normalized against β-actin and LaminA/C, respectively. (C) Nuclear extracts of cells were prepared and tested for the DNA-binding activities using the TransAM™ NF-κB family transcription factor assay kit (Student's t-test, **P<0.01). (D) The cell proliferative activity between the MGC-803-sictrl and MGC-803-siTRAF3 cells was examined by CCK-8 assay at 24, 48 and 72 h (Student's t-test, **P<0.01). (E) A cell viability assay was carried out to detect the viability of the 2 established cell lines at 24, 48 and 72 h. The relative luciferase activity was detected among the 2 established cell lines. Significant differences are indicated (Student's t-test, **P<0.01). (F) The migratory ability of the MGC-803-sictrl and MGC-803-siTRAF3 cells was detected by Transwell migration assay. Upper panel, representative images of migrated cells between the 2 established cell lines were photographed under an inverted microscope (x20 magnification). Bottom panel, the number of migrated cells was quantified (Student's t-test, **P<0.01). (G) The invasive ability of the MGC-803-sictrl and MGC-803-siTRAF3 cells was detected by Transwell invasion assay. Upper panel, representative images of invaded cells between the 2 established cell lines were photographed under an inverted microscope (x20 magnification). Bottom panel, the number of invaded cells was quantified (Student's t-test, **P<0.01).

with the control or *miR-17-92* plasmid. As shown in Fig. 6E, the atopic expression of the *miR-17-92* cluster significantly reduced the relative luciferase activity of the wild-type 3'-UTR of *TRAF3* (P<0.001), but not that of the mutant 3'-UTR of *TRAF3*. Taken together, it was confirmed that TRAF3 was a direct target of *miR-17-92*, which could downregulate TRAF3 expression by directly binding to the 3'-UTR of *TRAF3*.

TRAF3-silencing promotes cellular proliferation and enhances migration and invasion abilities of MGC-803 cells in vitro. We
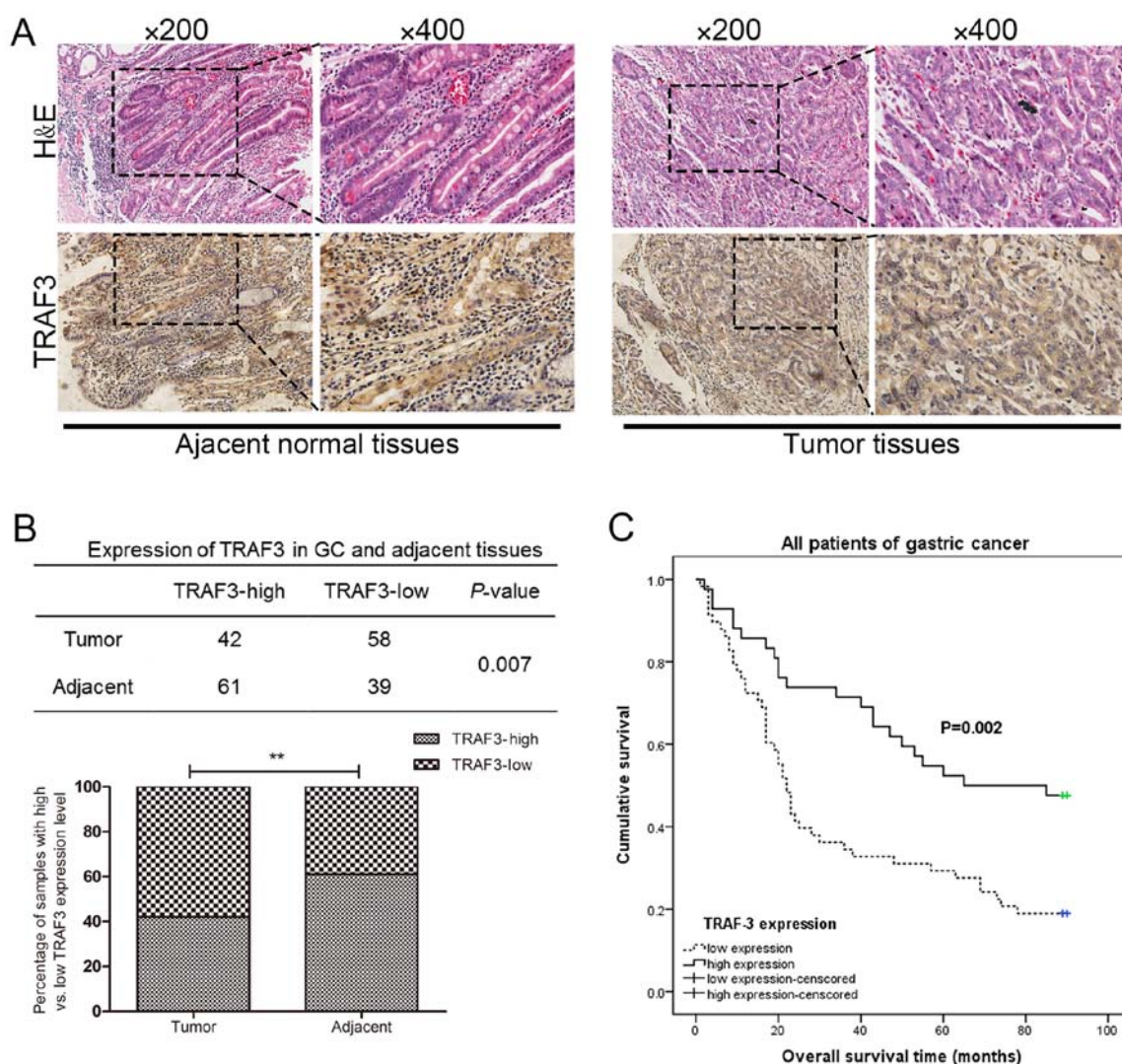
Figure 8. Tumor necrosis factor receptor associated factor 3 (TRAF3) functions as an important prognostic factor in patients with gastric cancer. (A) Representative images of TRAF3 protein expression levels between the gastric tumor tissues and the adjacent normal tissues from the microarray were determined by immuno-histochemistry. Original magnification: Left panels, x20; right panels, x40. (B) Upper panel, table showing the number of patients with high versus low TRAF3 expression between gastric tumors and adjacent normal tissues. Bottom panel, bar graph showing the percentage of samples with high versus low TRAF3 expression between gastric tumors and adjacent normal tissues. (C) Kaplan-Meier survival analysis of patients with gastric cancer according to the TRAF3 expression status. Kaplan-Meier analysis of cumulative survival in the low TRAF3 expression group (58 patients) and high TRAF3 expression group (42 patients). The P-value was based on the log-rank test. Patients with a low TRAF3 expression had a worse survival than those with a high TRAF3 expression (P=0.002).

further investigated whether TRAF3 functions as a target gene of the *miR-17-92* cluster in the MGC-803 cells. The MGC-803 cells were transfected with shRNA-TRAF3 or shRNA-control plasmid, respectively. As shown in Fig. 7A, both the mRNA and protein levels of TRAF3 were markedly lower in the MGC-803-siTRAF3 cells as compared with the MGC-803-sictrl cells, indicating a successful RNA interference (RNAi) of the *TRAF3* gene. The expression levels of RelA and p50 were clearly increased in the NE of the MGC-803-siTRAF3 cells compared to that in the MGC-803-sictrl cells. Moreover, the expression levels of RelB and p52 were upregulated in both the CE and NE in the MGC-803-siTRAF3 cells compared to that in the control cells (Fig. 7B). To further determine the exact contribution of TRAF3 silencing to the NF-κB DNA-binding capabilities in the MGC-803 cells, an ELISA-based NF-κB activity assay was performed. In line with the results of western blot analysis, the average DNA-binding capability of RelA, p50, RelB and p52 in the NE of the MGC-803-siTRAF3 cells were

significantly increased compared to that in the MGC-803-sictrl cells, while the DNA-binding capability of c-Rel remained unaltered (Fig. 7C). Therefore, TRAF3 silencing significantly activated not only canonical NF-κB activity, but also non-canonical NF-κB activity in the MGC-803 cells.

As shown by CCK-8 assay, the OD values at 450 nm in the MGC-803-siTRAF3 group (0.72±0.10, 1.71±0.20 and 2.14±0.17) were significantly higher than those in the MGC-803-sictrl group (0.64±0.13, 1.39±0.16 and 1.63±0.15) at 24, 48 and 72 h, respectively (all P<0.01, Fig. 7D). Moreover, a CellTiter-Glo cell viability assay was carried out. The relative luciferase activities of the MGC-803-sictrl cells were 110,886±17,428, 165,340±28,222 and 183,612±16,171 at 24, 48 and 72 h, respectively; while those in the MGC-803-siTRAF3 cells were 150,425±30,618, 224,387±31,175 and 241,320±24,341 at 24, 48 and 72 h, respectively (all P<0.01, Fig. 7E). Transwell migration and invasion assays were also performed. TRAF3 silencing markedly increased the number of migrated cells

Table I. Association between TRAF3 expression and clinicopathological characteristics of patients with gastric cancer.

Characteristics	No. of patients (n=100)	TRAF3 expression		P-value
		Low (n=58)	High (n=42)	
Age (years)				
Median	65 (32-81)			
≤65	51	29	22	0.814
>65	49	29	20	
Sex				
Male	64	37	27	0.960
Female	36	21	15	
Tumor diameter				
≤5 cm	52	25	27	0.036
>5 cm	48	33	15	
Site of tumor				
Cardia	13	5	8	0.325
Body	28	18	10	
Antrum	51	29	22	
Unknown	8	6	2	
Histological type				
Tubular adenocarcinoma	66	42	24	0.228
Mucinous adenocarcinoma	10	4	6	
Signet ring cell adenocarcinoma	11	7	4	
Undifferentiated carcinoma	13	5	8	
Tumor differentiation				
Well	15	6	9	0.219
Moderate	74	44	30	
Poor	11	8	3	
TNM stage				
I-II	42	18	24	0.009
III-IV	58	40	18	

Data were analyzed using the Chi-square test. A value of P<0.05 was considered to indicate a statistically significant difference.

approximately 3-fold in the MGC-803-siTRAF3 group as compared with the control group (P<0.01, Fig. 7F). Moreover, the number of cells that invaded the Matrigel layer from the MGC-803-siTRAF3 group was increased approximately ut 3-fold compared with that of the corresponding control group (P<0.01, Fig. 7G). Taken together, these results indicated that TRAF3 silencing promoted the proliferation, and enhanced the migratory and invasive abilities of the MGC-803 cells *in vitro*.

TRAF3 functions as an important prognosis factor in patients with human gastric cancer. The protein expression levels of TRAF3 in human gastric cancer tissues and adjacent normal tissues were detected by IHC analyses. As shown in Fig. 8A, the expression of TRAF3 could be clearly detected in both the nuclear and the cytoplasmic portions of the adjacent normal tissues. By contrast, the expression of TRAF3 was predominantly detected in the cytoplasm of the gastric tumor tissues.

Moreover, the expression of TRAF3 in the gastric tumor tissues was significantly lower than that in the adjacent normal gastric mucosa, and there was a statistically significance (P=0.007) between the gastric tumor tissues and the adjacent normal tissues (Fig. 8B). As shown in Table I, the association between TRAF3 expression and the clinicopathological characteristics in the 100 paired gastric cancer patients was evaluated. The expression of TRAF3 was negatively associated with tumor diameter and the TNM stage of patients with gastric cancer (P<0.05). The expression of TRAF3 was not associated with the other clinicopathological characteristics examined, including age, sex, site of tumor, histological types and tumor differentiation (P>0.05).

OS curves were also plotted according to TRAF3 expression using the Kaplan-Meier method. Survival analysis indicated that the low TRAF3 expression group had a significantly shorter OS rate than that of the high TRAF3 expression group, and there was a statistically significance (P=0.002) between

the low TRAF3 expression group and the high TRAF3 expression group (Fig. 8C). Taken together, these results indicated that TRAF3 expression was downregulated in gastric cancer tissues and that TRAF3 functions as an important prognosis factor in patients with gastric cancer.

Discussion

In this study, the role of the *miR-17-92* cluster in gastric cancer progression was systematically examined. The introduction of the *miR-17-92* overexpression plasmid into the MGC-803 human gastric cancer cells significantly promoted cell growth both *in vitro* and *in vivo*, which was predominantly due to the activation of the AKT, ERK and NF-κB signaling pathways. The migratory and invasive abilities of the cells were also promoted by the overexpression of the *miR-17-92* cluster, which was contributed to the occurrence of EMT. To the best of our knowledge, in this study, for the first time, TRAF3, a negative regulator of the NF-κB signaling pathway, was demonstrated to be a direct target of the *miR-17-92* cluster in the MGC-803 human gastric cancer cells. Of note, TRAF3 expression was indicative of a favorable prognosis factor of human gastric cancer patients.

In this study, we observed a significant and rapid growth rate of the MGC-803 cells due to the introduction of the *miR-17-92* cluster both *in vitro* and *in vivo*. Similar to the finding of previous studies, we demonstrated that *miR-17-92* overexpression significantly promoted cell growth due to increased cellular proliferation and decreased cellular apoptosis. As previously demonstrated, the increased expression of all the members of the *miR-17-92* cluster induced by the overexpression of E2F transcription factor 1 (E2F1) significantly promoted the proliferation of mouse palatal mesenchymal cells (31). The activation of the *miR-17-92* pathway is involved in the growth of small cell lung cancer due to the driving factor of the friend leukemia virus integration 1 (*FLI1*) gene (32). *In vivo*, the conditional deletion of *miR-17-92* in mouse pancreatic β-cells has been shown to significantly reduce the proliferative ability of pancreatic β-cells (33). *miR-17-5p* has been demonstrated to promote the proliferation of gastric cancer cells by targeting SOCS6 (21). Gain- and loss-of-function assays have also demonstrated that *miR-20a* affects the proliferative ability of uveal melanoma cells *in vitro* (34). The upregulation of *miR-18a* has been shown to promote cell proliferation by increasing Cyclin D1 expression by regulating PTEN-PI3K-AKT-mTOR signaling in esophageal squamous cell carcinoma cells (35). The overexpression of *miR-17* in gastric cancer cells is associated with several proliferation-associated oncogenes amplification, including *MYC*, *CCNE1*, *ERBB2* and *FGFR2*. The knockdown of *miR-17* suppresses the proliferative potential of KATO-III gastric cancer cells accompanied by the downregulation of p-ERK1/2 expression (22). Similarly, in this study, the expression of PTEN, which functions as a negative regulator of AKT signaling, was decreased upon the overexpression of the *miR-17-92* cluster in the MGC-803 cells. Correspondingly, we observed that the expression of p-AKT at Thr308 was induced without the level of total AKT being affected. The induction of p-ERK1/2 was also observed. These data confirm the function of the *miR-17-92* cluster in MGC-803 gastric cancer

cells with respect to cell proliferation, and the activation of the AKT and ERK signaling pathways are implicated in these processes. Furthermore, we found that the overexpression of the miR-17-92 cluster significantly promoted tumor growth *in vivo*. Therefore, we hypothesized that the activation of the AKT and ERK signaling pathways is important for the rapid tumor growth. Further studies are required to examine this hypothesis by analyzing these pathways in tumor tissues using assays, such as western blot analysis.

Furthermore, a number of studies have revealed the oncogenic activity of the *miR-17-92* cluster by regulating apoptotic genes. The overexpression of the *miR-17-92* cluster in DU145 prostate cancer cells has been shown to significantly decrease cellular apoptosis (29). *In vivo*, the overexpression of *miR-17-92* has been shown to block the induction of BIM-mediated apoptosis in multiple transgenic mouse models of acute lymphoblastic leukemia (36). In this study, we observed that *miR-17-92* overexpression in the MGC-803 cells resulted in the clear inhibition of cellular apoptosis due to the suppressed expression of BIM, which was a direct target of *miR-17-92*. As a pro-apoptotic protein, BIM regulates cell death by antagonizing anti-apoptotic proteins, such as Bcl-2 (37). The downregulation of PTEN expression can also contribute to the resistance to apoptosis. In myeloma cells, the overexpression of *miR-19a* has been shown to significantly inhibit cellular apoptosis and to function as an oncogenic miRNA by targeting the PTEN-AKT pathway (38). In response to various extracellular signals, the PI3K/AKT pathway participates in diverse cellular responses to promote cell survival, proliferation and cell growth. The NF-κB signaling pathway can be regulated by the *miR-17-92* cluster and regulates the balance between cellular proliferation and apoptosis (39,40). For example, *miR-17-92* contributes to chronic myeloid leukemia (CML) leukemogenesis by targeting A20 and activates NF-κB signaling (39). *miR-17-92* has been demonstrated to drive lymphomagenesis by suppressing the expression of multiple negative regulators of the PI3K and NF-κB pathways, and by inhibiting the mitochondrial apoptotic pathway (41). In this study, in the MGC-803 cells, both the canonical and non-canonical NF-κB signaling pathways were activated due to the overexpression of the *miR-17-92* cluster, which contributed to the regulation of multiple cellular functions, including cell proliferation and apoptosis.

Furthermore, in this study, we demonstrated that *miR-17-92* overexpression markedly promoted the migratory and invasive abilities of the MGC-803 cells. Our results are consistent with those of previous studies that the *miR-17-92* cluster plays an important role in cancer invasion and metastasis (42). The overexpression of the *miR-17-92* cluster in DU145 prostate cancer cells has been shown to promote cellular migration and invasion *in vitro* (29). *miR-17* facilitates the cell motility of melanoma cells by targeting ETV1 (43). *miR-19* plays an important role in the invasion and migration of lung cancer cells by modulating the EMT process (44). *miR-19a/b* promotes gastric cancer cell migration and invasion by targeting the antagonist of c-Myc-MXD1 (24). By contrast, Bahari *et al* reported that *miR-17-92* was downregulated in gastric cancer and that its expression was negatively associated with metastasis (45). In this study, we found that *miR-17-92* overexpression markedly enhanced the migratory and invasive abilities of the MGC-803

cells. The activation of NF-κB signaling in the MGC-803 cells overexpressing the *miR-17-92* cluster increased the expression of MMP-2, which is a downstream gene of the NF-κB signaling pathway. Of note, we demonstrated that there was a decrease in E-cadherin, EpCAM and Claudin1 expression levels coupled with an increase in N-cadherin and Vimentin expression levels in the MGC-803-miR-17-92 cells, indicating that EMT had occurred. EMT, which is characterized by the loss of epithelial characteristics and the acquisition of a mesenchymal phenotype, plays a critical role in allowing cancer cells to invade adjacent tissue and migrate to distant sites, where these cancer cells continue to proliferate and generate new tumors (46). Mounting evidence has indicatd that in epithelial cancers, including gastric cancer, the induction of EMT is a major event that provides mobility to cancer cells in order to generate metastasis (45). *miR-19* has been reported to trigger EMT in lung cancer cells, and thus enhances the migratory and invasive abilities of A549 and HCC827 cells (44). In this study, we demonstrated that *miR-17-92* overexpression promoted the migratory and invasive abilities of the MGC-803 gastric cancer cells, and the increased MMP-2 expression and the occurrence of EMT were implicated in these processes.

In mammals, the transcription factor family of NF-κB includes RelA/p65, NF-κB1/p50, RelB, NF-κB2/p52 and c-Rel. NF-κB subunits play important roles in cellular survival, inflammation, proliferation, apoptosis and tumorigenesis (47). TRAF3 is one of the most enigmatic members of the TRAF family with distinct cell and context-specific roles (48). TRAF3 is characterized to be an ubiquitin E3 ligase, and is mainly composed of a signature TRAF domain at the carboxyl terminus and a typical C3HC4 RING finger domain at the N-terminus (49). TRAF3 functions as an upstream regulator of NF-κB signaling, and suppresses NF-κB activity by constantly mediating the degradation of NF-κB-inducing kinase (NIK) (50). The downregulation of TRAF3 in NOD1 ligand-stimulated cells leads to enhanced NF-κB reporter activity, while it increases TRAF3 expression and suppresses NF-κB activity (51). In this study, we found that both the canonical and non-canonical NF-κB activities were activated in the MGC-803 gastric cancer cells due to the introduction of the *miR-17-92* cluster. We further observed that the overexpression of the *miR-17-92* cluster decreased TRAF3 expression at both the mRNA and protein level. Therefore, one possibility is that TRAF3 may be regulated by the *miR-17-92* cluster directly in MGC-803 cells. As a matter of fact, TRAF3 can be regulated by various miRNAs. For example, TRAF3 has been demonstrated to be targeted by *miR-32* to affect non-canonical NF-κB signaling and consequently, NIK stabilization (52). TRAF3 is also directly targeted by *miR-214-3p* to promote osteoclast- and bone-resorbing activity (53). In murine macrophages, *Burkholderia pseudomallei*-derived *miR-3473* has been shown to enhance NF-κB expression by targeting TRAF3 and is associated with different inflammatory responses compared to *Burkholderia thailandensis* (54). TRAF3 has also been demonstrated to be directly targeted by *miR-3178* (55), *miR-322* (56) and *miR-576-3p* (57). In this study, we used a luciferase reporter gene containing the 3'-UTR of the *TRAF3* gene to testify the direct repression of *TRAF3* by the *miR-17-92* cluster. Therefore, *miR-17-92* was able to bind to the complementary sites in the 3'-UTR of the

TRAF3 mRNA and regulate either its mRNA degradation or translational repression. In this study, we demonstrate that TRAF3 is a direct target of the *miR-17-92* cluster. Accordingly, the overexpression of the *miR-17-92* cluster in the MGC-803 cells caused a reduction in TRAF3-NF-κB signaling, which further influenced multiple cellular functions. To the best of our knowledge, this is the first study to demonstrate that *TRAF3* is regarded as a novel target of the *miR-17-92* cluster.

TRAF3 is ubiquitously expressed in the majority of tissues, including brain, heart, lung, liver and spleen. The expression pattern of TRAF3 in human gastric cancer tissue remains undefined. Zou *et al* demonstrated that the expression of TRAF3 was upregulated in *Helicobacter pylori*-positive gastric tissues but not in *Helicobacter pylori*-negative gastric tissues, and the expression of TRAF3 was also positive in both the intestinal and diffuse type gastric cancer samples (55). The clinicopathological analyses of 100 paired gastric cancer tissues from a tissue microarray was performed and the results suggested that TRAF3 expression was negatively associated with tumor diameter and TNM stage. Moreover, Kaplan-Meier survival analysis also revealed that a low expression of TRAF3 was associated with a shorter OS rate of patients with gastric cancer. Therefore, TRAF3 expression may be considered as a novel biomarker for the prognosis of patients with gastric cancer.

In conclusion, the findings of this study provide a key tumor-promoting role of the *miR-17-92* cluster in the development and progression of gastric cancer. The *miR-17-92* cluster plays an important role in cellular biological functions, including cell growth, proliferation, apoptosis, migration and invasion of MGC-803 gastric cancer cells. To the best of our knowledge, for the first time, we provide evidence that the *miR-17-92* cluster plays a pivotal role in regulating the NF-κB signaling pathway by directly targeting *TRAF3*. The miR-17-92/TRAF3/NF-κB axis may thus be a novel target for human gastric cancer therapy and may be further considered as a potential prognostic factor in the future.

Availability of data and materials

The datasets used and/or analyzed during the current study are available from the corresponding author on reasonable request.

Authors' contributions

WC and FG conceived and designed the study. Experimental procedures were conducted by FL, LC and JX. Data analysis was performed by LC. The manuscript was prepared by FL, and JX critically revised the manuscript. Financial support was obtained by WC, FG and JX. All authors have read and approved the final manuscript.

Ethics approval and consent to participate

The human tissues examined in this study were from a tissue microarray. All procedures involving animals and animal experiments were approved by the Animal Care and Use Committee of Soochow University.

Patient consent for publication

Not applicable.

Competing interests

The authors declare that they have no competing interests.

References

1. Torre LA, Bray F, Siegel RL, Ferlay J, Lortet-Tieulent J and Jemal A: Global cancer statistics, 2012. CA Cancer J Clin 65: 87-108, 2015.
2. Siegel RL, Miller KD and Jemal A: Cancer Statistics, 2017. CA Cancer J Clin 67: 7-30, 2017.
3. Bartel DP: MicroRNAs: Genomics, biogenesis, mechanism, and function. Cell 116: 281-297, 2004.
4. Bartel DP: MicroRNAs: Target recognition and regulatory functions. Cell 136: 215-233, 2009.
5. Zhang C: Novel functions for small RNA molecules. Curr Opin Mol Ther 11: 641-651, 2009.
6. Lujambio A and Lowe SW: The microcosmos of cancer. Nature 482: 347-355, 2012.
7. Esquela-Kerscher A and Slack FJ: Oncomirs - microRNAs with a role in cancer. Nat Rev Cancer 6: 259-269, 2006.
8. Tsai MM, Wang CS, Tsai CY, Huang HW, Chi HC, Lin YH, Lu PH and Lin KH: Potential diagnostic, prognostic and therapeutic targets of MicroRNAs in human gastric cancer. Int J Mol Sci 17: 17, 2016.
9. He L, Thomson JM, Hemann MT, Hernando-Monge E, Mu D, Goodson S, Powers S, Cordon-Cardo C, Lowe SW, Hannon GJ, *et al*: A microRNA polycistron as a potential human oncogene. Nature 435: 828-833, 2005.
10. Ota A, Tagawa H, Karnan S, Tsuzuki S, Karpas A, Kira S, Yoshida Y and Seto M: Identification and characterization of a novel gene, C13orf25, as a target for 13q31-q32 amplification in malignant lymphoma. Cancer Res 64: 3087-3095, 2004.
11. Hayashita Y, Osada H, Tatematsu Y, Yamada H, Yanagisawa K, Tomida S, Yatabe Y, Kawahara K, Sekido Y and Takahashi T: A polycistronic microRNA cluster, miR-17-92, is overexpressed in human lung cancers and enhances cell proliferation. Cancer Res 65: 9628-9632, 2005.
12. Farazi TA, Horlings HM, Ten Hoeve JJ, Mihailovic A, Halfwerk H, Morozov P, Brown M, Hafner M, Reyal F, van Kouwenhove M, *et al*: MicroRNA sequence and expression analysis in breast tumors by deep sequencing. Cancer Res 71: 4443-4453, 2011.
13. Chow TF, Mankaruos M, Scorilas A, Youssef Y, Girgis A, Mossad S, Metias S, Rofael Y, Honey RJ, Stewart R, *et al*: The miR-17-92 cluster is over expressed in and has an oncogenic effect on renal cell carcinoma. J Urol 183: 743-751, 2010.
14. Zhu H, Han C and Wu T: MiR-17-92 cluster promotes hepatocarcinogenesis. Carcinogenesis 36: 1213-1222, 2015.
15. Yu G, Tang JQ, Tian ML, Li H, Wang X, Wu T, Zhu J, Huang SJ and Wan YL: Prognostic values of the miR-17-92 cluster and its paralogs in colon cancer. J Surg Oncol 106: 232-237, 2012.
16. Li H, Wu Q, Li T, Liu C, Xue L, Ding J, Shi Y and Fan D: The miR-17-92 cluster as a potential biomarker for the early diagnosis of gastric cancer: Evidence and literature review. Oncotarget 8: 45060-45071, 2017.
17. Mogilyansky E and Rigoutsos I: The miR-17/92 cluster: A comprehensive update on its genomics, genetics, functions and increasingly important and numerous roles in health and disease. Cell Death Differ 20: 1603-1614, 2013.
18. Valladares-Ayerbes M, Blanco M, Haz M, Medina V, Iglesias-Díaz P, Lorenzo-Patiño MJ, Reboredo M, Santamarina I, Figueroa A, Antón-Aparicio LM, *et al*: Prognostic impact of disseminated tumor cells and microRNA-17-92 cluster deregulation in gastrointestinal cancer. Int J Oncol 39: 1253-1264, 2011.
19. Ren C, Wang W, Han C, Chen H, Fu D, Luo Y, Yao H, Wang D, Ma L, Zhou L, *et al*: Expression and prognostic value of miR-92a in patients with gastric cancer. Tumour Biol 37: 9483-9491, 2016.
20. Tsujiura M, Komatsu S, Ichikawa D, Shiozaki A, Konishi H, Takeshita H, Moriumura R, Nagata H, Kawaguchi T, Hirajima S, *et al*: Circulating miR-18a in plasma contributes to cancer detection and monitoring in patients with gastric cancer. Gastric Cancer 18: 271-279, 2015.
21. Wu Q, Luo G, Yang Z, Zhu F, An Y, Shi Y and Fan D: miR-17-5p promotes proliferation by targeting SOCS6 in gastric cancer cells. FEBS Lett 588: 2055-2062, 2014.
22. Park D, Lee SC, Park JW, Cho SY and Kim HK: Overexpression of miR-17 in gastric cancer is correlated with proliferation-associated oncogene amplification. Pathol Int 64: 309-314, 2014.
23. Wu W, Takanashi M, Borjigin N, Ohno SI, Fujita K, Hoshino S, Osaka Y, Tsuchida A and Kuroda M: MicroRNA-18a modulates STAT3 activity through negative regulation of PIAS3 during gastric adenocarcinogenesis. Br J Cancer 108: 653-661, 2013.
24. Wu Q, Yang Z, An Y, Hu H, Yin J, Zhang P, Nie Y, Wu K, Shi Y and Fan D: MiR-19a/b modulate the metastasis of gastric cancer cells by targeting the tumour suppressor MXD1. Cell Death Dis 5: e1144, 2014.
25. Wang F, Li T, Zhang B, Li H, Wu Q, Yang L, Nie Y, Wu K, Shi Y and Fan D: MicroRNA-19a/b regulates multidrug resistance in human gastric cancer cells by targeting PTEN. Biochem Biophys Res Commun 434: 688-694, 2013.
26. Wu Q, Yang Z, Wang F, Hu S, Yang L, Shi Y and Fan D: MiR-19b/20a/92a regulates the self-renewal and proliferation of gastric cancer stem cells. J Cell Sci 126: 4220-4229, 2013.
27. Pfaffl MW: A new mathematical model for relative quantification in real-time RT-PCR. Nucleic Acids Res 29: e45, 2001.
28. Liu F, Zhou J, Zhou P, Chen W and Guo F: The ubiquitin ligase CHIP inactivates NF-κB signaling and impairs the ability of migration and invasion in gastric cancer cells. Int J Oncol 46: 2096-2106, 2015.
29. Zhou P, Ma L, Zhou J, Jiang M, Rao E, Zhao Y and Guo F: miR-17-92 plays an oncogenic role and conveys chemo-resistance to cisplatin in human prostate cancer cells. Int J Oncol 48: 1737-1748, 2016.
30. Xu J, Zhou P, Wang W, Sun A and Guo F: RelB, together with RelA, sustains cell survival and confers proteasome inhibitor sensitivity of chronic lymphocytic leukemia cells from bone marrow. J Mol Med (Berl) 92: 77-92, 2014.
31. Li L, Shi B, Chen J, Li C, Wang S, Wang Z and Zhu G: An E2F1/MiR-17-92 Negative Feedback Loop mediates proliferation of Mouse Palatal Mesenchymal Cells. Sci Rep 7: 5148, 2017.
32. Li L, Song W, Yan X, Li A, Zhang X, Li W, Wen X, Zhou L, Yu D, Hu JF, *et al*: Friend leukemia virus integration 1 promotes tumorigenesis of small cell lung cancer cells by activating the miR-17-92 pathway. Oncotarget 8: 41975-41987, 2017.
33. Chen Y, Tian L, Wan S, Xie Y, Chen X, Ji X, Zhao Q, Wang C, Zhang K, Hock JM, *et al*: MicroRNA-17-92 cluster regulates pancreatic beta-cell proliferation and adaptation. Mol Cell Endocrinol 437: 213-223, 2016.
34. Zhou J, Jiang J, Wang S and Xia X: Oncogenic role of microRNA 20a in human uveal melanoma. Mol Med Rep 14: 1560-1566, 2016.
35. Zhang W, Lei C, Fan J and Wang J: miR-18a promotes cell proliferation of esophageal squamous cell carcinoma cells by increasing cylin D1 via regulating PTEN-PI3K-AKT-mTOR signaling axis. Biochem Biophys Res Commun 477: 144-149, 2016.
36. Li Y, Deutzmann A, Choi PS, Fan AC and Felsher DW: BIM mediates oncogene inactivation-induced apoptosis in multiple transgenic mouse models of acute lymphoblastic leukemia. Oncotarget 7: 26926-26934, 2016.
37. Gupta S, Read DE, Deepti A, Cawley K, Gupta A, Oommen D, Verfaillie T, Matus S, Smith MA, Mott JL, *et al*: Perk-dependent repression of miR-106b-25 cluster is required for ER stress-induced apoptosis. Cell Death Dis 3: e333, 2012.

38. Zhang X, Chen Y, Zhao P, Zang L, Zhang Z and Wang X: MicroRNA-19a functions as an oncogene by regulating PTEN/AKT/pAKT pathway in myeloma. Leuk Lymphoma 58: 932-940, 2017.
39. Jia Q, Sun H, Xiao F, Sai Y, Li Q, Zhang X, Yang S, Wang H, Wang H, Yang Y, et al: miR-17-92 promotes leukemogenesis in chronic myeloid leukemia via targeting A20 and activation of NF-κB signaling. Biochem Biophys Res Commun 487: 868-874, 2017.
40. Trenkmann M, Brock M, Gay RE, Michel BA, Gay S and Huber LC: Tumor necrosis factor α-induced microRNA-18a activates rheumatoid arthritis synovial fibroblasts through a feedback loop in NF-κB signaling. Arthritis Rheum 65: 916-927, 2013.
41. Jin HY, Oda H, Lai M, Skalsky RL, Bethel K, Shepherd J, Kang SG, Liu WH, Sabouri-Ghomi M, Cullen BR, et al: MicroRNA-17~92 plays a causative role in lymphomagenesis by coordinating multiple oncogenic pathways. EMBO J 32: 2377-2391, 2013.
42. Quattrochi B, Gulvady A, Driscoll DR, Sano M, Klimstra DS, Turner CE and Lewis BC: MicroRNAs of the mir-17~92 cluster regulate multiple aspects of pancreatic tumor development and progression. Oncotarget 8: 35902-35918, 2017.
43. Cohen R, Greenberg E, Nemlich Y, Schachter J and Markel G: miR-17 regulates melanoma cell motility by inhibiting the translation of ETV1. Oncotarget 6: 19006-19016, 2015.
44. Li J, Yang S, Yan W, Yang J, Qin YJ, Lin XL, Xie RY, Wang SC, Jin W, Gao F, et al: MicroRNA-19 triggers epithelial-mesenchymal transition of lung cancer cells accompanied by growth inhibition. Lab Invest 95: 1056-1070, 2015.
45. Bahari F, Emadi-Baygi M and Nikpour P: miR-17-92 host gene, uderexpressed in gastric cancer and its expression was negatively correlated with the metastasis. Indian J Cancer 52: 22-25, 2015.
46. Thiery JP, Acloque H, Huang RY and Nieto MA: Epithelial-mesenchymal transitions in development and disease. Cell 139: 871-890, 2009.
47. Gilmore TD: Introduction to NF-kappaB: Players, pathways, perspectives. Oncogene 25: 6680-6684, 2006.
48. He JQ, Oganesyan G, Saha SK, Zarnegar B and Cheng G: TRAF3 and its biological function. Adv Exp Med Biol 597: 48-59, 2007.
49. Arch RH, Gedrich RW and Thompson CB: Tumor necrosis factor receptor-associated factors (TRAFs)--a family of adapter proteins that regulates life and death. Genes Dev 12: 2821-2830, 1998.
50. Liao G, Zhang M, Harhaj EW and Sun SC: Regulation of the NF-kappaB-inducing kinase by tumor necrosis factor receptor-associated factor 3-induced degradation. J Biol Chem 279: 26243-26250, 2004.
51. Asano N, Imatani A, Watanabe T, Fushiya J, Kondo Y, Jin X, Ara N, Uno K, Iijima K, Koike T, et al: Cdx2 expression and intestinal metaplasia induced by H. pylori infection of gastric cells is regulated by NOD1-mediatedinnate immune responses. Cancer Res 76: 1135-1145, 2016.
52. Malcomson FC, Willis ND, McCallum I, Xie L, Lagerwaard B, Kelly S, Bradburn DM, Belshaw NJ, Johnson IT and Mathers JC: Non-digestible carbohydrates supplementation increases miR-32 expression in the healthy human colorectal epithelium: A randomized controlled trial. Mol Carcinog 56: 2104-2111, 2017.
53. Liu J, Li D, Dang L, Liang C, Guo B, Lu C, He X, Cheung HY, He B, Liu B, et al: Osteoclastic miR-214 targets TRAF3 to contribute to osteolytic bone metastasis of breast cancer. Sci Rep 7: 40487, 2017.
54. Fang Y, Chen H, Hu Y, Li Q, Hu Z, Ma T and Mao X: Burkholderia pseudomallei-derived miR-3473 enhances NF-κB via targeting TRAF3 and is associated with different inflammatory responses compared to Burkholderia thailandensis in murine macrophages. BMC Microbiol 16: 283, 2016.
55. Zou M, Wang F, Jiang A, Xia A, Kong S, Gong C, Zhu M, Zhou X, Zhu J, Zhu W, et al: MicroRNA-3178 ameliorates inflammation and gastric carcinogenesis promoted by Helicobacter pylori new toxin, Tip-α, by targeting TRAF3. Helicobacter 22: 22, 2017.
56. Gu H, Yu J, Dong D, Zhou Q, Wang JY and Yang P: The miR-322-TRAF3 circuit mediates the pro-apoptotic effect of high glucose on neural stem cells. Toxicol Sci 144: 186-196, 2015.
57. Yarbrough ML, Zhang K, Sakthivel R, Forst CV, Posner BA, Barber GN, White MA and Fontoura BM: Primate-specific miR-576-3p sets host defense signalling threshold. Nat Commun 5: 4963, 2014.